Phospholipid Binding and Lecithin−Cholesterol Acyltransferase Activation Properties of Apolipoprotein A-I Mutants†

Paul Holvoet,*,‡ Zhian Zhao,‡ Berlinda Vanloo,§ Rita Vos,|| Els Deridder,‡ Ann Dhoest,‡ Josée Taveirne,§ Els Brouwers,‡ Eddy Demarsin,‡ Yves Engelborghs,|| Maryvonne Rosseneu,§ Désiré Collen,‡ and Robert Brasseur⊥

Center for Molecular and Vascular Biology, University of Leuven, B-3000 Leuven, Belgium, Department of Clinical Chemistry, A. Z. St.-Jan, Brugge, Belgium, Laboratory of Chemical and Biological Dynamics, University of Leuven, B-3000 Leuvenm, Belgium, and Centre de Biophysique Moléculaire Numérique, Faculté de Sciences Agronomiques de Gembloux, Belgium

Received June 9, 1995; Revised Manuscript Received August 21, 1995⊗

ABSTRACT: Recombinant human apolipoprotein A-I (apo A-I) and three deletion mutants: apo A-I(ΔLeu^{44}−Leu^{126}), apo A-I(ΔGlu^{139}−Leu^{170}), and apo A-I(ΔAla^{190}−Gln^{243}), purified from the periplasmic space of *Escherichia coli*, were studied. The rate of turbidity decrease following mixing of apo A-I(ΔAla^{190}−Gln^{243}) with dimyristoylphosphatidylcholine (DMPC) vesicles at 23 °C was 10-fold lower than that of the other apo A-I proteins, confirming that the carboxy-terminal region of apo A-I plays a role in rapid lipid binding. The Stokes radii of reconstituted high-density lipoproteins (rHDL), containing dipalmitoylphosphatidylcholine and cholesterol, were larger for the three apo A-I mutants [6.3 nm for apo A-I(ΔLeu^{44}−Leu^{126}), 6.1 nm for apo A-I(ΔGlu^{139}−Leu^{170}), and 6.5 nm for apo A-I(ΔAla^{190}−Gln^{243})] than for intact apo A-I (5.0 nm). The mutant rHDL all contained 4 apo A-I molecules per particle as compared to 2 for intact apo A-I. Circular dichroism measurements revealed 8 α-helices per apo A-I molecule, 5 per apo A-I(ΔLeu^{44}−Leu^{126}), 6 per apo A-I(ΔGlu^{139}−Leu^{170}), and 4 per apo A-I(ΔAla^{190}−Gln^{243}) molecule as compared to predicted values of 8, 5, 6, and 6 α-helices, respectively. The catalytic efficiencies for activation of lecithin−cholesterol acyltransferase (LCAT) were 2-fold lower for apo A-I(ΔLeu^{44}−Leu^{126}), 11-fold lower for apo A-I(ΔGlu^{139}−Leu^{170}), and 8-fold lower for apo A-I(ΔAla^{190}−Gln^{243}) than for intact apo A-I, as a result of a significant decrease of V_{max} but not of K_m values. In aggregate, these data suggest that deletion of the amino-terminal or of the central domains of apo A-I has little effect on lipid binding, whereas deletion of the carboxy-terminal domain reduces the rate but not the extent of lipid binding. Furthermore, deletion of the central domain [in apo A-I(ΔGlu^{139}−Leu^{170})] or conformational modifications in the central domain [in apo A-I(ΔAla^{190}−Glu^{243})] result in a decrease of the rate of LCAT activity that is independent of the binding of LCAT to rHDL.

Low plasma levels of high-density lipoproteins (HDL)[1] and of their major protein component, apolipoprotein A-I (apo A-I), correlate with an increased risk for coronary heart disease (Gordon & Rifkind, 1989), and family and twin studies have suggested that decreased HDL levels are partially heriditary (Christian et al., 1990; De Backer et al., 1986; Hunt et al., 1989; Pometta et al., 1979). In addition, HDL and their apolipoproteins increase the net efflux of cellular unesterified cholesterol (Daniels et al., 1981; Fielding & Fielding, 1981; Oram et al., 1981), and remove excess cholesterol from peripheral (nonhepatic) cells (Glomset, 1968), which may explain the inverse correlation between risk of coronary heart disease and HDL levels (Miller et al., 1985).

Cholesterol esterification, a requirement for its transport from peripheral cell membranes to the liver, is catalyzed by LCAT, a reaction that is greatly stimulated by apo A-I (Fielding et al., 1972). LCAT plays a role not only in the reesterification of HDL cholesterol but also in the regulation of the HDL level, as suggested by the greatly decreased HDL levels in familial LCAT deficiency (Funke et al., 1991a) and in fish-eye disease (Funke et al., 1991b).

Apo A-I is synthesized as a prepropeptide; it is cotranslationally cleaved to pro-apo A-I, and during secretion cleaved to form the mature 243 amino acid apo A-I protein (Brewer et al., 1978). Folding of apo A-I into amphipathic helices composed of hydrophilic and hydrophobic surfaces (Segrest et al., 1974, 1990, 1992) has been demonstrated using complexes of phospholipids with plasma apo A-I and with model peptides (Anantharamaiah et al., 1985; Fukushima et al., 1980; Kroon et al., 1978; Nakagawa et al., 1985;

† This study was supported by the Nationaal Fonds voor Wetenschappelijk Onderzoek (Project 3.0063.94).

* Correspondence should be addressed to this author at the Center for Molecular and Vascular Biology, University of Leuven, Campus Gasthuisberg, O & N Herestraat 49, B-3000 Leuven, Belgium. Telephone: 32-16-34.57.72. Fax: 32-16-34.59.90.

‡ Center for Molecular and Vascular Biology, University of Leuven.

§ A. Z. St.-Jan.

|| Laboratory of Clinical and Biological Dynamics, University of Leuven.

⊥ Faculté de Sciences Agronomiques de Gembloux.

⊗ Abstract published in *Advance ACS Abstracts,* October 1, 1995.

[1] Abbreviations: apo A-I, apolipoprotein A-I; apo A-I(ΔLeu^{44}−Leu^{126}), apo A-I mutant with the Leu^{44}−Leu^{126} segment deleted; apo A-I(ΔGlu^{139}−Leu^{170}), apo A-I mutant with the Glu^{139}−Leu^{170} segment deleted; apo A-I(ΔAla^{190}−Gln^{243}), apo A-I mutant with the Ala^{190}−Gln^{243} segment deleted; DMPC, dimyristoylphosphatidylcholine; DPPC, dipalmitoylphosphatidylcholine; EDTA, ethylenediaminetetraacetic acid; HDL, high-density lipoproteins; rHDL, reconstituted high-density lipoproteins; LCAT, lecithin−cholesterol acyltransferase; CD, circular dichroism; FPLC, fast performance liquid chromatography; HPLC, high-performance liquid chromatography; SDS−PAGE, sodium dodecyl sulfate−polyacrylamide gel electrophoresis.

0006-2960/95/0434-13334$09.00/0

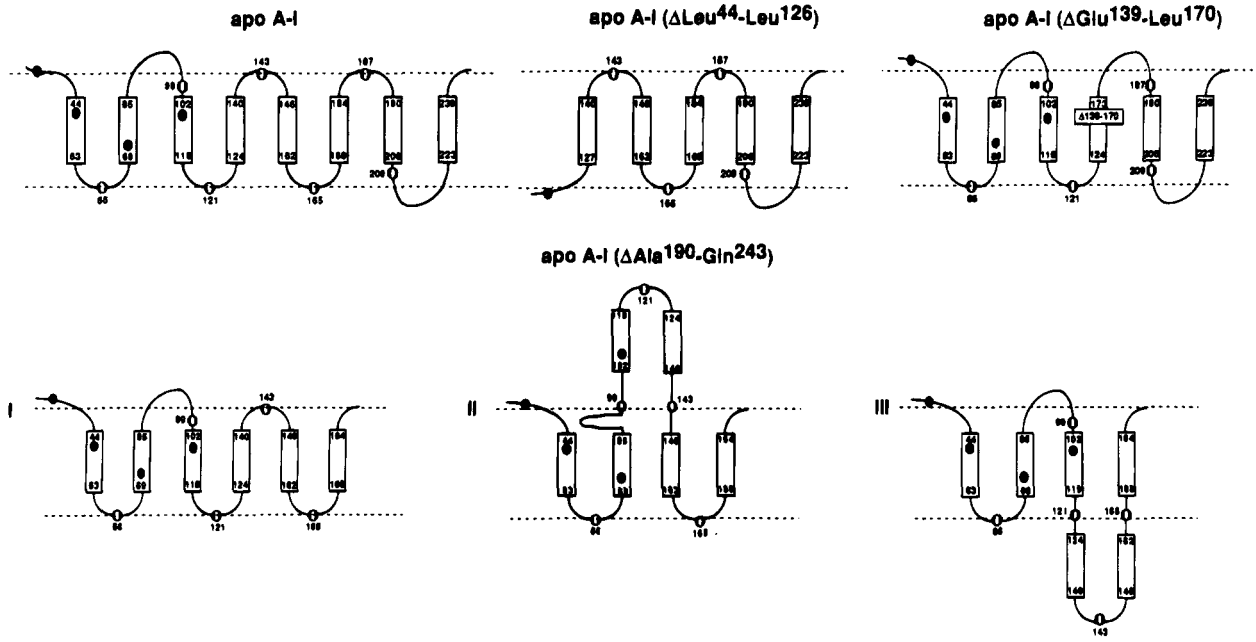

FIGURE 1: Schematic representation of the secondary structure of apo A-I proteins in rHDL. Open circles represent proline residues in β-strands and closed circles tryptophan residues in the amino-terminal domain of apo A-I that are contributing to the fluorescence properties. For apo A-I(ΔAla^{190}–Gln^{243}), three possible conformations are illustrated: (I) with 6 helices bound to the edge of the disc; (II) with 4 helices bound to the edge of the disc and a hinged domain located between residues Asn^{102} and Lys^{140}; or (III) with 4 helices bound to the edge of the disc and a hinged domain located between residues Ala^{124} and His^{162}.

Sparrow & Gotto, 1980; Srinivas et al., 1991; Vanloo et al., 1991). Based upon energy minimization calculations and infrared spectroscopy measurements, a general model was proposed for the association of apo A-I and phospholipids in discoidal complexes (Brasseur, 1991; Brasseur et al., 1990; Wald et al., 1990). According to this model, apo A-I contains 8 putative amphipathic α-helices that are oriented parallel to the acyl chains of the phospholipids, around the edge of the discs, with their hydrophobic surface toward the lipid core and with their hydrophilic surface toward the aqueous phase (Figure 1). The first amino-terminal domain (residues 44–63) has the lowest helical structure probability, while the second helix (residues 69–85) is not involved into a pair (Brasseur, 1991; Brasseur et al., 1990). The 6 carboxy-terminal helical structures most likely form pairs of antiparallel α-helices stabilized by protein–protein interactions. A minimum length of 17–20 amino acids (5–6 helical turns) appears to be required for effective phospholipid binding and LCAT activation (Brasseur, 1991; Brasseur et al., 1990). However, the domains of apo A-I involved in phospholipid binding and/or LCAT activation remain unidentified. Two naturally occurring mutants, one with a deletion of Lys^{107} (Rall et al., 1984) and one with a substitution of Pro^{143} with Arg (Utermann et al., 1984), have a 50% reduced ability to activate LCAT. Minnich et al. (1992) found that although binding of apo A-I(ΔGlu^{113}–Ala^{124}), apo A-I(ΔMet^{148}–Gly^{186}), and apo A-I(ΔAsp^{213}–Gln^{243}) to liposomes was 50–80% of normal, the two latter apo A-I mutants surprisingly did not form discoidal complexes. LCAT activation with these mutants was 47%, 0.5%, and 13% of normal. For apo A-I(ΔAsp^{213}–Gln^{243}), this was found to be due to a 15-fold reduction of the K_m value, suggesting decreased binding of LCAT to the multilamellar vesicles obtained with this mutant. Sorci-Thomas et al. (1993) found that the binding of apo A-I(ΔPro^{99}–Gly^{120}), apo A-I(ΔPro^{143}–Ala^{164}), and apo A-I(ΔPro^{220}–Asn^{241}) to unilamellar vesicles was normal, but their LCAT activity was reduced 10-fold. However, from these data it was not clear whether the reduced LCAT activation was due to reduced V_{max} or to increased K_m. Furthermore, because the composition of the complexes and the conformation of the apo A-I proteins in the respective complexes were not studied, it could not be excluded that reduced LCAT activation was due to conformational differences instead of deletion of a domain that is critical for LCAT interaction. However, Jonas et al. (1989) have previously demonstrated that conformational changes of intact apo A-I in larger discoidal rHDL, with decreased α-helical contents, already are associated with a 20-fold decrease of LCAT activation. Recently, Schmidt et al. demonstrated that deletion of the carboxy-terminal domain of apo A-I resulted in decreased in vivo lipoprotein association and thus in an increased clearance rate (Schmidt et al., 1995).

In the present study, three mutants of apo A-I were selected in which putative phospholipid binding and/or LCAT activation domains were deleted. The three first amino-terminal α-helical repeats, overlapping with the putative LCAT-activating domain proposed by Anantharamaiah et al. (1990), were deleted in apo A-I(ΔLeu^{44}–Leu^{126}) (Figure 1). The central (Glu^{146}–His^{162}) α-helix, with its adjacent β-strands, overlapping the Gly^{145}–Ala^{164} putative LCAT activation domain (Sparrow & Gotto, 1980), was deleted in apo A-I(ΔGlu^{139}–Leu^{170}) (Figure 1). Finally, the two carboxy-terminal α-helical repeats, overlapping the putative phospholipid binding Thr^{197}–Gly^{245} fragment that by itself could not activate LCAT (Sparrow & Gotto, 1980; Soutar et al., 1975), were deleted in apo A-I(ΔAla^{190}–Gln^{243}) (Figure 1). In this study, we demonstrate that deletion of the Ala^{190}–Gln^{243} carboxy-terminal domain from apo A-I reduces its rate of phospholipid binding, but does not prevent discoidal complex formation. Furthermore, deletion of the Glu^{139}–Leu^{170} central domain or the Ala^{190}–Gln^{243} carboxy-terminal domain but not of the Leu^{44}–Leu^{126} amino-terminal domain results in a disruption of conformation of the apo A-I central domain and in a decrease of the rate of LCAT activation that is independent of LCAT binding.

EXPERIMENTAL PROCEDURES

Oligonucleotide-Directed Mutagenesis and DNA Sequencing. All DNA manipulations were carried out essentially as described by Maniatis et al. (1982). Oligonucleotide-directed mutagenesis was performed by the gapped-duplex method of Kramer et al. (1984) using the *pMa/c* vector system of Stanssens et al. (1989). This system employs phasmid (i.e., phage/plasmid hybrid) vectors allowing cloning and site-directed mutagenesis as well as sequencing to be carried out in the same vector without recloning. Oligonucleotides were obtained by custom synthesis (Pharmacia, Brussels, Belgium). DNA sequences were determined using a primer walking strategy on a Pharmacia ALF DNA sequencer (Pharmacia, Uppsala, Sweden). Template DNA was purified by alkaline hydrolysis followed by a poly(ethylene glycol) precipitation step. The sequencing reactions were carried out using T7 DNA polymerase (Pharmacia) and a fast denaturation protocol as described elsewhere (Zhou et al., 1990). The reaction products were sized on 6% Hydrolink Long Ranger gels (AT Biochem, Malvern, PA) containing 1× TBE buffer and run with 0.6× TBE buffer. The sequence was assembled using the IntelliGenetics Suite 5.4 program (IntelliGenetics, Palo Alto, CA).

Construction of cDNA for Expression of Wild-Type Apo A-I and Apo A-I Mutants. The *pMc-5-apo A-I* transfection vector, encoding wild-type recombinant apo A-I, for expression in *E. coli* under control of the *tac*-promoter and the *PhoA* signal peptide sequence was constructed starting from the plasmid *pA1-3* (Cheung & Chan, 1983), the *pUC-19* vector (Yanisch-Perron et al., 1985), and the *pMa/c* mutagenesis vector (Stanssens et al., 1989). The plasmid *pA1-3*, obtained by insertion of the *apo A-I* cDNA in the *Pst*I site of pBR322 (Cheung & Chan, 1983), was a kind gift of Dr. L. Chan, Baylor College of Medicine (Houston, TX).

The 961 bp *Pst*I fragment from *pA1-3*, comprising the entire coding region and the signal peptide sequence of apo A-I, was ligated in the *Pst*I-treated *pUC-19* vector, resulting in the *pUC-apo A-I* vector. The 1010 bp *Kpn*I−*Hin*dIII fragment from *pUC-apo A-I* was ligated in the *Kpn*I- and *Hin*dIII-treated *pMc-5* vector, resulting in the *pMc-5-int* vector, containing both the *PhoA signal peptide* and the *apo A-I signal peptide* coding sequences. A 43 bp fragment, dGATGAACCACCACAGAGTCCATGGGATCGAGTGAAGGATCTGG, was inserted in the *Kpn*I (blunt-ended)−MscI-treated *pMc-5-int*, resulting in the *pMc-5-apo A-I* vector, in which the *apo A-I signal peptide* coding sequence was deleted. In addition, in order to increase the efficiency of mutagenesis, 5 silent mutations were simultaneously introduced in the 43 bp apo A-I coding sequence: the CCC codons for Pro^3, Pro^4, and Pro^7 were replaced with CCA; the AGC codon for Ser^6 was replaced with AGT; and the GAC codon for Asp^{13} was replaced with GAT. The *pMc-5-apo A-I* cDNA thus expressed wild-type apo A-I under the control of the *tac*-promoter in *E. coli* (Figure 2).

Deletion mutagenesis with the 47-mer deoxynucleotide dAGCTTCTGGCGCGCCCTCTTGGTT CAGCTGTTTTCCCAAGGCGGA was performed on the *pMc-5-apo A-I* vector to delete the Leu^{44}−Leu^{126} coding sequence, resulting in the *pMC-5-apo A-I*(ΔLeu^{44}−Leu^{126}) vector for expression of apo A-I(ΔLeu^{44}−Leu^{126}) in *E. coli* (Table 1).

Deletion mutagenesis with the 36-mer oligodeoxynucleotide dGGCCAAGCGCTGGCGTTGCAGCT CGTGAAGCTTCTG was performed on the *pMc-5-apo A-I* vector to delete the Glu^{139}−Leu^{170} sequence, resulting in the *pMc-5-Apo A-I*(ΔGlu^{139}−Leu^{170}) vector for expression of apo A-I(ΔGlu^{139}−Leu^{170}) in *E. coli*. By substitution of the CTG codon for Leu^{134} with the CTT codon for Leu, an additional *Hin*dIII restriction site was created (Table 1).

Deletion mutagenesis wih the 48-mer oligodeoxynucleotide dGGAAGGTGGGCGACGGCGAGCGCCTCACAGT CTGGCACCACCGTTCTC was performed on the *pMc-5-apo A-I* vector to delete the Ala^{190}−Gln^{243} coding sequence, resulting in the *pMc-5-apo A-I* (ΔAla^{190}−Gln^{243}) vector for expression of apo A-I(ΔAla^{190}−Gln^{243}) in *E. coli* (Table 1).

All cDNA constructs were confirmed by DNA sequencing.

Expression in E. coli and Cell Fractionation. E. coli WK6 host cells were grown in 2YT medium to an optical density at 600 nm of approximately 0.4, at which point isopropyl-β-D-thiogalactopyranoside was added to a final concentration of 0.4 mM. Cells were further incubated at 37 °C for 2 h, during which the optical cell density increased to 10^{12} cells/L. The cell suspensions (10 L) were centrifuged at 10000*g* for 10 min, the supernatant was removed, and periplasmic cell fractions were prepared as described previously (Koshland & Botstein, 1980). The pellet is treated with 70 mL of 0.02 M Tris·HCl, pH 8.2, containing 27% sucrose. Thereafter, 800 μL of 0.5 M EDTA and 4 mL of a 2 mg/mL lysozyme solution are added. The mixture is incubated for 30 min on ice. Thereafter 1.2 mL of 1 M $CaCl_2$ is added. Finally, the pellet is centrifuged for 15 min, the supernatant is harvested, and $(NH_4)_2SO_4$ is added to a final concentration of 1 M.

Purification. All proteins were purified to homogeneity by a combination of hydrophobic interaction chromatography, ion-exchange chromatography on Q-Sepharose, and gel filtration. The supernatant is applied to a 2.5 × 12 cm phenyl-Sepharose column. Bound apo A-I proteins were eluted by applying a 1−0 M $(NH_4)_2SO_4$ gradient (total volume 190 mL). Apo A-I proteins, assessed in ELISA, eluted at 0.1−0.15 M salt. The apo A-I-containing fractions were pooled, dialyzed against 0.02 M Tris·HCl, pH 8.2, containing 7 M urea, and applied to a 2.5 × 6 cm Q-Sepharose column. Bound apo A-I proteins were eluted by applying a 0−0.1 M NaCl gradient (total volume 100 mL). Apo A-I proteins eluted at 0.04−0.06 M salt. The apo A-I-containing fractions were concentrated with PEG 20 000 and applied to a 1.6 × 60 cm Superdex 75 Prep Grade column, equilibrated with 0.02 M Tris·HCl, pH 8.2, containing 0.15 M NaCl.

Circular Dichroism Spectrometry. Circular dichroism spectra of lipid-free apo A-I proteins in solution and of apo A-I proteins in discoidal apo A-I/phospholipid/cholesterol complexes were measured at increasing temperatures with a Jasco J600 spectropolarimeter (Japan Spectroscopy, Tokyo, Japan) at wavelengths between 200 and 250 nm, using 6 μM sample solutions and a 1 mm path length cuvette. Temperatures were increased from 25 to 85 °C at a rate of 3 °C/5 min. Backgrounds were measured at 250 nm for 5 min, followed by measurements of the α-helical content at 222 nm for 5 min. For all apo A-I proteins, the α-helical content could be restored upon cooling of the solutions overnight. The fraction of α-helices in the secondary structure of the apo A-I proteins was estimated from the molar ellipticities at 222 nm ($[\theta]_{222} = (-30\,300 \times f_H) - 2340$) where f_H is the fraction of α-helical structure (Chen et al., 1972).

DMPC−Apo A-I Assembly. Kinetic turbidimetric measurements were carried out as described by Pownall et al.

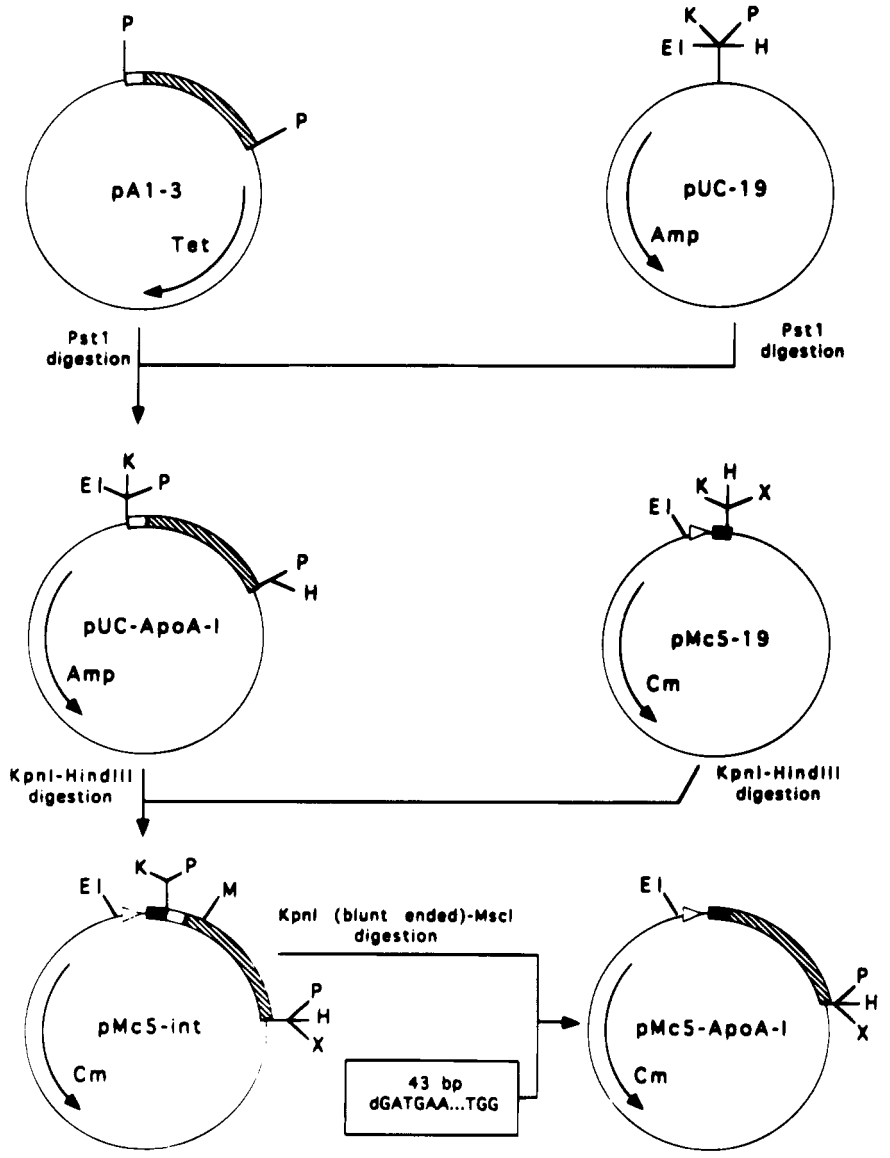

FIGURE 2: Construction of the *pMc-5-apo A-I* transfection vector. The 961 bp *Pst*I fragment from *pA1-3* was ligated in the *Pst*I-treated *pUC-19* vector, resulting in the *pUC-apo A-I* vector. The 1010 bp *Kpn*I−*Hin*dIII fragment from *pUC-apo A-I* was ligated in the *Kpn*I- and *Hin*dIII-treated *pMc-5*, resulting in the *pMc-5-int* vector, containing both the *PhoA* signal peptide and the *apo A-I* signal peptide coding sequences. A 43 bp fragment, dGATGAACCACCACAGAGTCCATGGGATCGAGTGAAGGATCTGG, was inserted in the *Kpn*I (blunt-ended)−*Msc*I-treated *pMc-5-int* vector, resulting in the *pMc-5-Apo A-I* vector. In this cloning step, the *apo A-I* signal peptide coding sequence was removed. In addition, 5 silent mutations were simultaneously introduced, as described under Experimental Procedures. Hatched boxes represent the mature *apo A-I* cDNA sequence, open boxes the *apo A-I* signal peptide, black boxes the *PhoA* signal peptide, and open triangles the *tac* promoter. Restriction endonucleases indicated are as follows: EI, *Eco*RI; H, *Hin*dIII; K, *Kpn*I; M, *Msc*I; P, *Pst*I; X, *Xba*I.

(1981). DMPC and apo A-I proteins were dissolved at molar concentrations of 600 and 6 μM in 0.01 M Tris·HCl buffer, pH 7.4, containing 8.5% KBr, 0.01% sodium azide, and 0.01% EDTA and incubated at 23 °C for 10 min before mixing of equal volumes of the reagents. The lipid−protein association was followed by monitoring the rate of disappearance of liposomal turbidity at 325 nm. Pownall et al. (1981) defined a rate constant $k_{1/2} = 1/t_{1/2}$, where $t_{1/2}$ is the time required for the decrease of half of the relative turbidity $[(A_0 - A_\infty)/A_0]$.

Preparation of Discoidal Apo A-I/DPPC/Cholesterol Complexes. Complexes of the apo A-I proteins with dipalmitoylphosphatidylcholine (DPPC, Sigma) and cholesterol, at an apo A-I/DPPC/cholesterol ratio of 1/3/0.15 (w/w/w), were prepared using the cholate dialysis procedure (Matz & Jonas, 1982; Vanloo et al., 1991). The mixture was incubated at 43 °C for 16 h, and cholate was removed by extensive dialysis. Complexes were isolated by gel filtration on a Superose 6 HR column equilibrated with 20 mM Tris·HCl buffer, pH 8.1, containing 0.15 M NaCl and 0.02 mg/mL sodium azide, in a FPLC system (Waters). One milliliter fractions were collected. The size of these complexes was estimated by comparison of their migration position on native 4−15% gradient polyacrylamide gels with that of standard proteins: thyroglobulin (Stokes radius of 8.5 nm), apoferritin (6.1 nm), catalase (5.2 nm), and lactate dehydrogenase (4.1 nm) (Pharmacia). The number of apo A-I molecules per lipoprotein particle was determined following cross-linking of apo A-I with bis(sulfosuccinimidyl) suberate (final concentration 1 mM) for 1 h, as previously described (Swaney, 1986), and separation of cross-linked proteins by SDS−PAGE on 4−15% gradient gels. The extent of oligomer formation was estimated by comparison with cross-linked plasma apo A-I (Swaney, 1986). The chemical composition of the isolated complexes was assayed as follows: the levels of phospholipid and

cholesterol were determined using commercial enzymatic kits (Biomérieux, France, for phospholipid; Boehringer Mannheim, Germany, for cholesterol), and the concentrations of apo A-I were determined according to Bradford (1976).

Fluorescence Analysis. Corrected steady-state fluorescence spectra and intensities were obtained on a SPEX spectrofluorometer (Fluorolog 1691). Excitation was carried out at 295 nm where the contribution of tyrosyl fluorescence to the total intensity is minimal. Fluorescence was measured with a 2 mm slit width in quartz cuvettes with optical path lengths equal to 1 and 0.4 cm and wavelength resolutions of 7.2 and 3.6 nm for the emission and the excitation wavelengths, respectively. Excitation was vertically polarized and fluoresence detected with a polarizer at a 54° angle to reduce the influence of the fluorescence depolarizatoin and Brownian motion on the detected intensity. The spectra were corrected for the wavelength dependence of the emission monochromator and the photomultiplier and for background intensities as described previously (Roberts, 1981). In the fluorescence quenching experiments, the spectra were recorded at increasing concentrations of KI. The results were analyzed by the Stern−Volmer equation as modified by Lehrer (Lehrer, 1971): $F_0/(F_0 - F) = 1/f_a + (1/f_aK_{SV})(1/[KI])$, where F_0 and F are the fluorescence intensities oberved in the absence or in the presence of a given concentration of KI, respectively, and f_a is the fraction of quenchable fluorescence (Jonas et al., 1993). The Stern−Volmer constant, K_{SV}, is an index of the accessibility of tryptophan residues to the aqueous phase.

Purification of LCAT. LCAT was purified 5100-fold from plasma and ultracentrifuged at densities of 1.21 and 1.25 g/mL, by chromatography on Affi-Gel Blue and DEAE-Sephadex (Matz & Jonas, 1982). Remaining impurities (65% of total protein), detected by SDS−PAGE electrophoresis and immunoblotting, essentially consisted of albumin. The enzyme was dialyzed against 10 mM Tris·HCl buffer, pH 7.6, containing 5 mM EDTA, and solutions were stored at −80 °C.

Kinetics of LCAT Activation by Discoidal Apo A-I/DPPC/Cholesterol Complexes. LCAT activation by discoidal apo A-I/DPPC/cholesterol complexes was monitored by incubation of the equivalent of 10−40 μM unesterified cholesterol, with a final concentration of 50 nM LCAT (Vercaemst et al., 1989). The reaction was carried out in 10 mM Tris.HCl buffer, pH 8.0, containing 5 mM EDTA, 0.15 M NaCl, 4−16 mg/mL delipidated bovine serum albumin and 6 mM β-mercaptoethanol. After preincubation for 20 min at 37 °C, LCAT was added. The mixture was incubated at 37 °C for 10−180 min, whereafter the reaction was arrested by extraction of cholesteryl esters with hexane/2-propanol (3/2, v/v) containing cholesteryl heptadecanoate as an internal standard. Under these reaction conditions, less than 20% of the cholesterol was esterified. Generated cholesteryl esters were quantified by isocratic HPLC on a reversed-phase ZORBAX ODS column, eluted with acetonitrile/2-propanol (50/50, v/v), as described previously (Vercaemst et al., 1989). Initial activation rates were obtained from plots of the concentration of generated cholesteryl esters versus time, and the kinetic parameters, K_m (expressed in micromolar cholesterol) and V_{max} (expressed in nanomoles of cholesteryl esters generated per hour), were determined by linear regression analysis from Lineweaver−Burk plots.

Table 1: Amino Acid Compositions and Molecular Masses of Intact Apo A-I and Apo A-I Mutants

compound	no. of amino acids	mol mass[a] (kDa)	mol mass[b] (kDa)
plasma apo A-I	243	28	28
recombinant apo A-I	243	28	28
apo A-I(ΔLeu^{44}−Leu^{126})	160	18	18.4
apo A-I(ΔGlu^{139}−Leu^{170})	211	24.4	24.1
apo A-I(ΔAla^{190}−Gln^{243})	189	22	21.7

[a] Molecular mass calculated on the basis of the amino acid composition. [a] Molecular mass calculated from the migration distance on 10−15% SDS−polyacrylamide gels.

FIGURE 3: SDS−PAGE of purified apo A-I proteins on 10−15% gradient gels. Proteins (5 μg per lane) were stained with Coomassie Brilliant Blue. Lane 1, plasma apo A-I; lane 2, recombinant apo A-I; lane 3, apo A-I(ΔLeu^{44}−Leu^{126}); lane 4, apo A-I(ΔGlu^{139}−Leu^{170}); lane 5, apo A-I(ΔAla^{190}−Gln^{243}); and lane 6, protein calibration mixture consisting of phosphorylase *b* (M_r 94 kDa), albumin (M_r 67 kDa), ovalbumin (M_r 43 kDa), carbonic anhydrase (M_r 30 kDa), trypsin inhibitor (M_r 20 kDa), and α-lactalbumin (M_r 14.4 kDa).

RESULTS

The predicted secondary structure of apo A-I (Brasseur et al., 1990; Brasseur, 1991) is illustrated in Figure 1. The predicted number of α-helices per molecule are 8 for intact apo A-I, 5 for apo A-I(ΔLeu^{44}−Leu^{126}), 6 for apo A-I(ΔGlu^{139}−Leu^{170}), and 6 for apo A-I(ΔAla^{190}−Gln^{243}).

Wild-type apo A-I and the apo A-I mutants (Table 1) were expressed in the periplasmic space of *E. coli* cells, and purified to homogeneity as evidenced by their migration as single bands on 10−15% SDS−polyacrylamide gels (Figure 3). Wild-type apo A-I migrated at exactly the same position as plasma apo A-I. Molecular masses of the apo A-I mutants, calculated from a plot of the logarithm of the molecular mass of the standard proteins vs the migration distance, were 18.4 kDa for apo A-I(ΔLeu^{44}−Leu^{126}), 24.1 kDa for apo A-I(ΔGlu^{139}−Leu^{170}), and 21.7 kDa for apo A-I(ΔAla^{190}−Gln^{243}) (Table 1), and thus were in agreement with those calculated on the basis of the respective amino acid compositions.

The rates of turbidity decrease following mixing of apo A-I moieties with DMPC vesicles (Table 2) were 10-fold lower for apo A-I(ΔAla^{190}−Gln^{243}) than for plasma apo A-I, recombinant apo A-I, apo A-I(ΔLeu^{44}−Leu^{126}), or apo A-I(ΔGlu^{139}−Leu^{170}), suggesting that the Ala^{190}−Gln^{243} domain is determining the rate of lipid binding. However, with apo A-I(ΔAla^{190}−Gln^{243}) as with the other apo A-I proteins, more than 85% of the turbidity was cleared, thus suggesting that the extent of phospholipid binding was not affected by the deletion of the carboxy-terminal domain.

Table 2: Rate Constants for Decrease of Turbidity following Mixing of Apo A-I Proteins with DMPC[a]

compound	$k_{1/2}$ (min^{-1})
plasma apo A-I	0.20 ± 0.01
recombinant apo A-I	0.19 ± 0.01
apo A-I(ΔLeu^{44}−Leu^{126})	0.22 ± 0.03
apo A-I(ΔGlu^{139}−Leu^{170})	0.17 ± 0.02
apo A-I(ΔAla^{190}−Gln^{243})	0.02 ± 0.002

[a] The data represent means ± SD of 3 independent determinations.

The α-helical contents for the different apo A-I proteins in aqueous solution, as determined by CD scanning, were 48% for apo A-I, 40% for apo A-I(ΔLeu^{44}−Leu^{126}), 45% for apo A-I(ΔGlu^{139}−Leu^{170}), and 48% for apo A-I(ΔAla^{190}−Gln^{243}). SDS-PAGE of apo A-I proteins in aqueous solution, cross-linked at 6 μM final concentrations with bis(sulfosuccinimidyl) suberate, revealed <25% oligomers for all apo A-I proteins (not shown). These data suggested that the decrease of the rate of phospholipid binding of apo A-I(ΔAla^{190}−Gln^{243}) was not due to increased self-association.

Discoidal apo A-I/DPPC/cholesterol complexes were obtained with all apo A-I proteins. Recoveries of apo A-I proteins in discoidal complexes after gel filtration were 90% for wild-type apo A-I (fractions 22−30 with maximum at fraction 27), 80% for apo A-I(ΔLeu^{44}−Leu^{126}) (fractions 18−28 with maximum at fraction 23), and 70% for apo A-I(ΔGlu^{139}−Leu^{170}) (fractions 18−30 with maximum at fraction 25) and for apo A-I(ΔAla^{190}−Gln^{243}) (fractions 18−28 with maximum at fraction 21). Top fractions (4 mL) were further analyzed. The apo A-I/phospholipid/cholesterol molar ratios, calculated from the measured protein, phospholipid, and cholesterol levels, were 1/110/10 for intact apo A-I (identical for plasma apo A-I and recombinant apo A-I), 1/80/10 for apo A-I(ΔLeu^{44}−Leu^{126}), and 1/80/12 for both apo A-I(ΔGlu^{139}−Leu^{170}) and apo A-I(ΔAla^{190}−Gln^{243}). The complex particles obtained with the three apo A-I mutants had similar sizes but were larger than those obtained with intact apo A-I, whereas the sizes of the complexes obtained with plasma apo A-I and recombinant apo A-I were identical (Figure 4, Table 3). Cross-linking of the apo A-I molecules within the discoidal apo A-I/DPPC/C particles revealed 4 apo A-I molecules per particle for all apo A-I mutant rHDL as compared to 2 for intact apo A-I (Figure 5, Table 3). The phospholipid surface was calculated from the circumference of the disc using the measured diameter minus 3 nm, i.e., 2 × radius of an α-helix, multiplied with a height of the disc of 3.8 nm. The number of phospholipid molecules was calculated from the calculated surface divided by 0.45 nm^2, the surface area per condensed phospholipid molecule. The calculated apo A-I/phospholipid molar ratios were 1/108 for intact apo A-I, 1/75 for apo A-I(ΔLeu^{44}−Leu^{126}), 1/71 for apo A-I(ΔGlu^{139}−Leu^{170}), and 1/79 for apo A-I(ΔAla^{190}−Gln^{243}), respectively, and were thus in agreement with the ratios calculated on the basis of the composition of the rHDL.

The α-helical contents of the apo A-I proteins in discoidal apo A-I/DPPC/cholesterol complexes were 74% for apo A-I, 75% for apo A-I(ΔLeu^{44}−Leu^{126}), 60% for apo A-I(ΔGlu^{139}−Leu^{170}), and 52% for apo A-I(ΔAla^{190}−Gln^{243}). Thus, numbers of α-helices per apo A-I molecule, calculated from the α-helical content determined by CD scanning and from the protein length assuming a length of 22 amino acids per α-helical repeat (Brasseur et al., 1990; Segrest et al., 1974), were 8 for intact apo A-I, 5 for apo A-I(ΔLeu^{44}−Leu^{126}), 6 for apo A-I(ΔGlu^{139}−Leu^{170}), and 4 for apo A-I(ΔAla^{190}−Gln^{243}) (Table 3). These values are in agreement with the predicted values (Brasseur et al., 1990) for intact apo A-I, apo A-I(ΔLeu^{44}−Leu^{126}), and apo A-I(ΔGlu^{139}−Leu^{170}), but are lower for apo A-I(ΔAla^{190}−Gln^{243}) (Table 3). The T_m values, i.e., temperature values at which the α-helical content is reduced by 50%, were 68, 68, 65, and 62 °C, respectively, further indicating that stable complexes were obtained with all apo A-I proteins. The fractions of the phospholipid surfaces that are covered by α-helix were calculated as the total phospholipid surface divided by 4 nm^2, the surface area of an α-helix that contains 16 amino acids. The calculated fractions were 0.77 for intact apo A-I, 0.70 for apo A-I(ΔLeu^{44}−Leu^{126}), and 0.87 for apo A-I(ΔGlu^{139}−Leu^{170}), but only 0.53 for apo A-I(ΔAla^{190}−Gln^{243}) (Table 3).

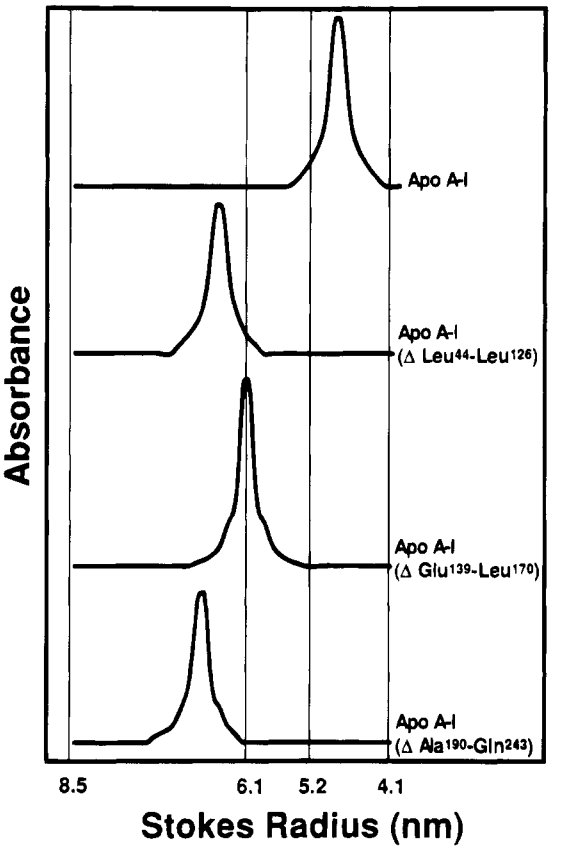

FIGURE 4: Determination of Stokes radii of rHDL by native polyacrylamide gel scanning. rHDL particles, isolated by gel filtration on a Superose 6HR column, were subjected to electrophoresis on 4−15% gradient polyacrylamide gels under nondenaturing conditions. The protein calibration mixture contained thyroglobulin (Stokes radius of 8.5 nm), apoferritin (6.1 nm), catalase (5.2 nm), and lactate dehydrogenase (4.1 nm). Because the sizes of plasma apo A-I and recombinant apo A-I rHDL were identical, only the gel scan for recombinant apo A-I rHDL is presented.

Binding of all apo A-I proteins to DPPC was associated with a shift of the Trp fluorescence maxima to lower wavelengths from 337 to 332 nm for intact apo A-I (both for plasma apo A-I and for recombinant apo A-I), from 338 to 329 nm for apo A-I(ΔLeu^{44}−Leu^{126}), from 339 to 333 nm for apo A-I(ΔGlu^{139}−Leu^{170}), and from 335 to 332 nm for apo A-I(ΔAla^{190}−Gln^{243}) (Table 4), suggesting that lipid binding is associated with translocation of Trp residues to a more apolar environment. The quenching parameters K_{SV} and f_a are summarized in Table 4. For totally exposed Trp residues, in the absence of electrostatic or viscosity effects, K_{SV} = 12 M^{-1} and f_a = 1, whereas for totally protected Trp

Table 3: Properties of Discoidal Apo A-I/DPPC/Cholesterol Complexes

properties	compound			
	apo A-I[g]	apo A-I-(ΔLeu^{44}–Leu^{126})	apo A-I-(ΔGlu^{139}–Leu^{170})	apo A-I-(ΔAla^{190}–Gln^{243})
Stokes radius (nm)[a]	5.0	6.3	6.1	6.5
apo A-I molecules per disc (n)[b]	2	4	4	4
α-helical content (%)[c]	74	75	60	52
α-helices per apo A-I molecule (n)[d]	8	5	6	4
estimated no. of a-helices per apo A-I (n)[e]	8	5	6	6
fraction of phospholipid surface covered with α-helices[f]	0.77	0.70	0.87	0.53

[a] Size of rHDL particles determined by PAGE. [b] The number of apo A-I molecules per rHDL particle was determined by SDS–PAGE after cross-linking with bis(sulfosuccinimidyl) suberate. [c] The α-helical content was determined by CD scanning. [d] The numbers of α-helices per apo A-I molecule were calculated from c and from the protein length assuming a length of 16 amino acids for the amphipathic helices and 6 amino acids for the adjacent β-strands (Brasseur et al., 1990; Segrest et al., 1974). [e] Estimated number according to the model of Brasseur et al. (1990) (Figure 1). [f] The phospholipid surface was calculated from the circumference of the disc, using the measured diameter minus 3 nm, multiplied by the height of the disc of 3.8 nm. The area covered by an α-helix containing 16 amino acids was estimated to be 4 nm^2. [g] Values for plasma apo A-I and recombinant apo A-I were identical.

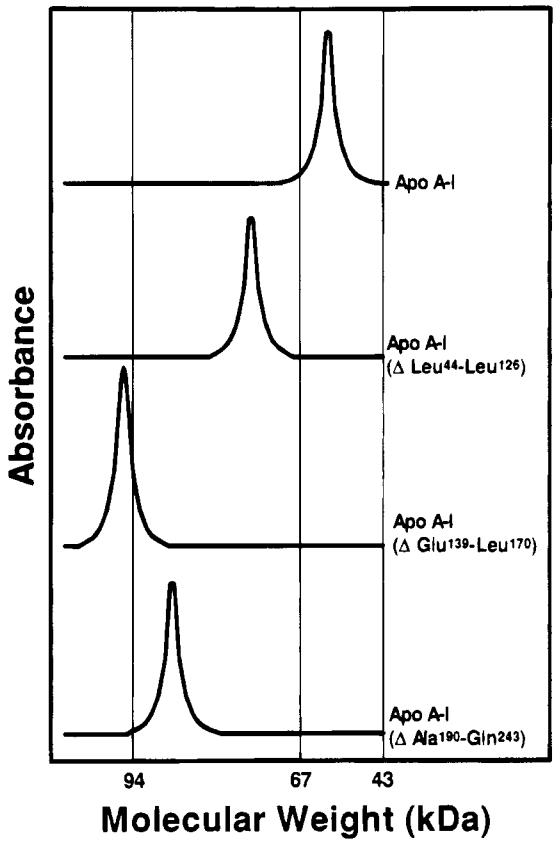

FIGURE 5: Determination of the number of apo A-I molecules per rHDL particle by SDS–polyacrylamide gel scanning. rHDL particles, in which apo A-I molecules were cross-linked with bis(sulfosuccinimidyl) suberate, were subjected to electrophoresis on 10–15% gradient SDS–polyacrylamide gels. The protein calibration mixture contained phosphorylase b (M_r 94 kDa), albumin (M_r 67 kDa), and ovalbumin (M_r 43 kDa). Because both plasma apo A-I and recombinant apo A-I produced rHDL particles that contained 2 apo A-I molecules per particle, only the gel scan for recombinant apo A-I is presented.

residues $K_{SV} = 0$ and $f_a = 0$. The K_{SV} values were 3 M^{-1} for intact apo A-I (both plasma and recombinant apo A-I), apo A-I(ΔGlu^{139}–Leu^{170}), and apo A-I(ΔAla^{190}–Gln^{243}) (Table 4) in rHDL as compared to 8 M^{-1} for the apo A-I proteins free in solution, indicating that the accessibility of the Trp residues to the aqueous phase in the respective rHDL is reduced to the same extent. The K_{SV} value for apo A-I(ΔLeu^{44}–Leu^{126}) in rHDL was 5 M^{-1} and thus somewhat higher than for the other apo A-I proteins. However, apo A-I(ΔLeu^{44}–Leu^{126}) contains only the Trp^8 residue, and thus its fluorescence properties cannot be directly compared with those of the other apo A-I proteins. The f_a values for the single Trp^8 residue in apo A-I(ΔLeu^{44}–Leu^{126}) were not different from the f_a values calculated for the other apo A-I proteins that all contain 4 Trp residues per molecule, thus indicating that the quenchable fluorescence represented on average 60% of the total fluorescence (Table 4) for all apo A-I proteins in rHDL.

LCAT activation by all discoidal apo A-I/DPPC/cholesterol complexes obeyed Michaelis–Menten kinetics, as shown by linear Lineweaver–Burk plots of the inverse of the initial activation rate ($1/v_0$) versus the inverse of the cholesterol concentrations (1/[C]). The apparent kinetic parameters V_{max} and K_m and the V_{max}/K_m ratios for the different apo A-I/DPPC/cholesterol complexes are summarized in Table 5. Deletion of the Glu^{139}–Leu^{170} and Ala^{190}–Gln^{243} domains resulted in a 11-fold and 10-fold decrease, respectively, of the apparent catalytic efficiency for LCAT activation, whereas deletion of the Leu^{44}–Leu^{126} domain produced a 2-fold decrease. The differences in LCAT activation were due to differences in V_{max} but not in K_m.

DISCUSSION

In the present study, lipid binding of three deletion mutants of apo A-I, apo A-I(ΔLeu^{44}–Leu^{126}), apo A-I(ΔGlu^{139}–Leu^{170}), and apo A-I(ΔAla^{190}–Gln^{243}), was studied. Deletion of the Ala^{190}–Gln^{243} carboxy-terminal domain, but not of the Leu^{44}–Leu^{126} amino-terminal or the Glu^{139}–Leu^{170} central domains, resulted in a 10-fold slower interaction with phospholipids. However, the extent of in vitro phospholipid binding was similar for all apo A-I proteins, as demonstrated by comparable disc formation after mixing the apo A-I proteins and phospholipids at equal weight ratios. This was evidenced by a shift of the maximum Trp fluorescence to a shorter wavelength and by decreased accessibility of its Trp residues to I$^-$. The sizes of rHDL constituted with apo A-I(ΔAla^{190}–Gln^{243}), apo A-I(ΔLeu^{44}–Leu^{126}), and apo A-I(ΔGlu^{139}–Leu^{170}) were larger than those with intact apo A-I. Furthermore, all mutant rHDL contained 4 apo A-I molecules per particle as compared to 2 for intact apo A-I. Circular dichroism scanning revealed 8 α-helices per intact apo A-I molecule, 5 per apo A-I(ΔLeu^{44}–Leu^{126}), 6 per apo A-I(ΔGlu^{139}–Leu^{170}), and 4 per apo A-I(ΔAla^{190}–Gln^{243}) molecule, as compared to the predicted numbers (Brasseur et al., 1990) of 8, 5, 6, and 6 α-helices, respectively. As the interaction of apolipoproteins with fluid interfaces is

Table 4: Fluorescence Properties of Apo A-I Proteins in rHDL Particles[a]

properties	compound: apo A-I[b]	apo A-I-(ΔLeu^{44}−Leu^{126})	apo A-I-(ΔGlu^{139}−Leu^{170})	apo A-I-(ΔAla^{190}−Gln^{243})
wavelength of max fluorescence (nm)	332	329	333	332
Stern−Volmer constant, K_{SV} (M^{-1}), for quenching of Trp fluorescence with I^-	2.9 ± 0.7	5.1 ± 0.5[c]	3.1 ± 1.1	3.4 ± 1.2
quenchable fraction of Trp fluorescence (f_a)	0.61 ± 0.08	0.62 ± 0.05	0.59 ± 0.01	0.58 ± 0.06

[a] Data represent means ± SD for 3 independent preparations. [b] Values for plasma apo A-I and recombinant apo A-I were identical. [c] Apo A-I(ΔLeu^{44}−Leu^{126}) only contains the Trp^8 residue and not the Trp^{50}, Trp^{72}, and Trp^{108} residues.

Table 5: Apparent Kinetic Parameters for the Reaction of LCAT with rHDL Particles[a]

compound	app V_{max} (nmol of CE/h)	app K_m (μM)	app V_{max}/app K_m [nmol of CE/(h·μM)]
plasma apo A-I	6.0	12	0.50
recombinant apo A-I	6.2	14	0.44
apo A-I(ΔLeu^{44}−Leu^{126})	2.7	11	0.20
apo A-I(ΔGlu^{139}−Leu^{170})	0.44	11	0.04
apo A-I(ΔAla^{190}−Gln^{243})	0.59	13	0.05

[a] Data represent mean values for 2 independent measurements. V_{max} and K_m are derived from linear ($r = 0.99$) Lineweaver−Burk plots of $1/v_0$ vs 1/[C] with [C] ranging from 10 to 40 μM. LCAT concentration was 50 nM.

driven by increased helix formation, the reduced α-helical content of apo A-I(ΔAla^{190}−Gln^{243}) is indicative of an altered conformation of this mutant in rHDL.

The LCAT activities of both apo A-I(ΔGlu^{139}−Leu^{170}) and apo A-I(ΔAla^{190}−Gln^{243}) were approximately 10-fold lower, whereas the activity of apo A-I(ΔLeu^{44}−Leu^{126}) was only 2-fold lower than that of intact apo A-I. Although LCAT activation may be sensitive to the size of the rHDL particles (Barter et al., 1985; Dobiasova et al., 1991, 1992), this alone cannot explain the differences in LCAT activity. Indeed, whereas apo A-I(ΔLeu^{44}−Leu^{126}) rHDL particles are larger than intact apo A-I rHDL particle, their LCAT activities are very similar. Furthermore, whereas the sizes of the two other mutant rHDL particles are similar to that of the first mutant rHDL particle, their LCAT activities are significantly lower. Furthermore, differences in apo A-I/phospholipid ratios cannot explain the differences in LCAT activity. Therefore, the data suggest that deletion of the Glu^{139}−Leu^{170} or the Ala^{190}−Gln^{243} segments results in disruption of a critical domain for LCAT activation. Domains in apo A-I that are critical for LCAT activation may, by analogy with the lipoprotein lipase/colipase system, contain regions which mediate the binding of LCAT to the lipoprotein particle. Alternatively, they may contain regions that "activate" the lipid substrates by promoting the correct orientation of the *sn*-2 ester bond of phosphatidylcholine for presentation to the catalytic site of the enzyme and orientating the cholesterol molecule within the surface monolayer in such a way that its esterification is promoted. Finally, they may contain regions that activate LCAT following a protein to protein interaction that results in a conformational change in the enzyme (Dolphin, 1992). In the present study, the differences in LCAT activity appeared to be due to changes in the apparent V_{max} values, which reflect the activated enzyme concentration, and not to differences in K_m, which are a function of the affinity of LCAT for rHDL (Bolin & Jonas, 1994). Thus, these data suggest that deletion of the Glu^{139}−Leu^{170} or of the Ala^{190}−Gln^{243} domains may disrupt a critical conformation of the central domain of apo A-I that is required for optimal phospholipid and cholesterol presentation to the enzyme (Sparks et al., 1995). The reduced α-helical content of apo A-I(ΔAla^{190}−Gln^{243}) in rHDL (as compared to the predicted conformation I) and the 30% reduction of the phospholipid surface that in the resulting rHDL particles is covered with α-helices (Table 3) are in agreement with alternative conformations of apo A-I(ΔAla^{190}−Gln^{243}) in rHDL. These differences are supporting the existence of a hinged domain overlapping the Asn^{102}−Lys^{140} segment (Figure 1, conformation II) or overlapping the Ala^{124}−His^{162} segment (Figure 1, conformation III). The existence in apo A-I of a hinged domain, constituted by a pair of central α-helices, such as those located between residues Pro^{99} and Leu^{143} or Pro^{121} and Pro^{165}, has been proposed to explain the discontinuous sizes observed in HDL particles (Brouillette et al., 1984; Cheung et al., 1987) or the differences in immunoreactivity of monoclonal antibodies with lipid-free and lipid-bound forms of apo A-I (Calabresi et al., 1993; Meng et al., 1993). Similar structures have also been suggested by Breiter et al. (1991), on the basis of the X-ray determination of the structure of an insect apolipoprotein of 18−20 kDa referred to as apolipoprotein III (Shapiro et al., 1988). The fluorescence properties of apo A-I(ΔAla^{190}−Gln^{243}), showing that both the K_{SV} and f_a values are not different from those of intact apo A-I, support more conformation III than conformation II. Recently an N-terminal proteolytic fragment of apo A-I was found to form rHDL with sizes and size distributions distinct from those of intact apo A-I rHDL (Ji & Jonas, 1995) but with 6 α-helices per apo A-I molecule in contact with POPC phospholipids. The finding that these rHDL retained the ability to activate LCAT further suggests that the carboxy-terminal fragment of apo A-I is not necessary for the specific activation of LCAT but that differences in the LCAT activity of different rHDL produced with the same apo A-I proteins may rather be due to conformational changes of these apo A-I proteins in rHDL resulting from differences in composition.

In conclusion, the present data suggest that any mutation in apo A-I that results in a disruption of the conformation of its central domain results in reduced LCAT activity.

ACKNOWLEDGMENT

Dr. R. Brasseur is a senior scientist in the "Fonds de la Recherche Scientifique de Belgique". Dr. R. Vos is a research associate of the Nationaal Fonds voor Wetenschappelijk Onderzoek. We thank G. Vanderheeren (Interdisciplinary Research Center, University of Leuven at Kortrijk, Belgium) for the CD measurements.

REFERENCES

Anantharamaiah, G. M., Jones, J. L., Brouillette, C. G., Schmidt, C. F., Chung, B. H., Hughes, T. A., Bhown, A. S., & Segrest, J. P. (1985) *J. Biol. Chem. 260*, 10248−10255.

Anantharamaiah, G. M., Venkatachalapathi, Y. V., Brouillette, C. G., & Segrest, J. P. (1990) *Arteriosclerosis 10*, 95−105.
Barter, P. J., Hopkins, G. J., & Gorjatschko, L. (1985) *Atherosclerosis 58*, 97−107.
Bolin, D. J., & Jonas, A. (1994) *J. Biol. Chem. 269*, 7429−7434.
Bradford, M. M. (1976) *Anal. Biochem. 72*, 248−254.
Brasseur, R. (1991) *J. Biol. Chem. 266*, 16120−16127.
Brasseur, R., De Meutter, J., Vanloo, B., Goormaghtigh, E., Ruysschaert, J. M., & Rosseneu, M. (1990) *Biochim. Biophys. Acta 1043*, 245−252.
Breiter, D. R., Kanost, M. R., Benning, M. M., Wesenberg, G., Law, J. H., Wells, M. A., Rayment, I., & Holden, H. M. (1991) *Biochemistry 30*, 603−608.
Brewer, H. B., Jr., Fairwell, T., LaRue, A., Ronan, R., Houser, A., & Bronzert, T. J. (1978) *Biochem. Biophys. Res. Commun. 80*, 623−630.
Brouillette, C. G., Jones, J. L., Ng, T. C., Kercret, H., Chung, B. H., & Segrest, J. P. (1984) *Biochemistry 23*, 359−367.
Calabresi, L., Meng, Q. H., Castro, G. R., & Marcel, Y. L. (1993) *Biochemistry 32*, 6477−6484.
Chen, Y. H., Yang, J. T., & Martinez, H. M. (1972) *Biochemistry 11*, 4120−4131.
Cheung, P., & Chan, L. (1983) *Nucleic Acids Res. 11*, 3703−3715.
Cheung, M. C., Segrest, J. P., Albers, J. J., Cone, J. T., Brouillette, C. G., Chung, B. H., Kashyap, M., Glasscock, M. A., & Anantharamaiah, G. M. (1987) *J. Lipid Res. 28*, 913−929.
Christian, J. C., Carmelli, D., Castelli, W. P., Fabsitz, R., Grim, C. E., Meaney, F. J., Norton, J. A. Jr., Reed, T., Williams, C. J., & Wood, P. D. (1990) *Arteriosclerosis 10*, 1020−1025.
Daniels, R. J., Guertler, L. S., Parker, T. S., & Steinberg, D. (1981) *J. Biol. Chem. 256*, 4978−4983.
De Backer, G., Hulstaert, F., De Munck, K., Rosseneu, M., Van Parijs, L., & Dramaix, M. (1986) *Am. Heart J. 112*, 478−484.
Dobiasova, M., Stribrna, J., Sparks, D. L., Pritchard, P. H., & Frohlich, J. J. (1991) *Arterioscler. Thromb. 11*, 64−70.
Dobiasova, M., Stribrna, J., Pritchard, P. H., & Frohlich, J. J. (1992) *J. Lipid Res. 83*, 1411−1418.
Dolphin, P. J. (1992) in *Structure and Function of Apolipoprotein* (Rosseneu, M., Ed.) pp 295−362, CRC Press, Boca Raton, FL.
Fielding, C. J., & Fielding, P. E. (1981) *Proc. Natl. Acad. Sci. U.S.A. 78*, 3911−3914.
Fielding, C. J., Shore, V. G., & Fielding, P. E. (1972) *Biochem. Biophys. Res. Commun. 46*, 1493−1498.
Fukushima, D., Yokoyama, S., Kroon, D. J., Kezdy, F. J., & Kaiser, E. T. (1980) *J. Biol. Chem. 255*, 10651−10657.
Funke, H., von Eckardstein, A., Pritchard, P. H., Albers, J. J., Kastelein, J. J., Droste, C., & Assmann, G. (1991a) *Proc. Natl. Acad. Sci. U.S.A. 88*, 4855−4859.
Funke, H., von Eckardstein, A., Pritchard, P. H., Karas, M., Albers, J. J., & Assmann, G. (1991b) *J. Clin. Invest. 87*, 371−376.
Glomset, J. A. (1968) *J. Lipid Res. 9*, 155−167.
Gordon, D. J., & Rifkind, B. M. (1989) *N. Engl. J. Med. 321*, 1311−1316.
Hunt, S. C., Hasstedt, S. J., Kuida, H., Stults, B. M., Hopkins, P. N., & Williams, R. R (1989) *Am. J. Epidemiol. 129*, 625−638.
Ji, Y., & Jonas, A. (1995) *J. Biol. Chem. 270*, 11290−11297.
Jonas, A., Kézdy, K. E., & Wald, J. H. (1989) *J. Biol. Chem. 264*, 4818−4824.
Jonas, A., Steinmetz, A., & Churgay, L. (1993) *J. Biol. Chem. 268*, 1596−1602.
Koshland, D., & Botstein, D. (1980) *Cell 20*, 749−760.
Kramer, W., Drutsa, V., Jansen, H. W., Kramer, B., Pflugfelder, M., & Fritz, H. J. (1984) *Nucleic Acids Res. 12*, 9441−9456.
Kroon, D. J., Kupferberg, J. P., Kaiser, E., & Kezdy, F. J. (1978) *J. Am. Chem. Soc. 100*, 5975−5977.
Lehrer, S. S. (1971) *Biochemistry 10*, 3254−3263.
Maniatis, T., Fritsch, E. F., & Sambrook, J. (1982) in *Molecular Cloning (A Laboratory Manual)*, p 200, Cold Spring Harbor Laboratory, Cold Spring Harbor, NY.
Matz, C. E., & Jonas, A. (1982) *J. Biol. Chem. 257*, 4535−4540.
Meng, Q. H., Calabresi, L., Fruchart, J. C., & Marcel, Y. L. (1993) *J. Biol. Chem. 268*, 16966−16973.
Miller, N. E., La Ville, A., & Crook, D. (1985) *Nature 314*, 109−111.
Minnich, A., Collet, X., Roghani, A., Cladaras, C., Hamilton, R. L., Fielding, C. J., & Zannis, V. I. (1992) *J. Biol. Chem. 267*, 16553−16560.
Nakagawa, S. H., Lau, H. S. H., Kezdy, F. J., & Kaiser, E. T. (1985) *J. Am. Chem. Soc. 107*, 7087−7092.
Oram, J. F., Albers, J. J., Cheung, M. C., & Bierman, E. L. (1981) *J. Biol. Chem. 256*, 8348−8356.
Pometta, D., Micheli, H., Suenram, A., & Jornot, C. (1979) *Atherosclerosis 34*, 419−429.
Pownall, H., Pao, Q., Hickson, D., Sparrow, J. T., Kusserow, S. K., & Massey, J. B. (1981) *Biochemistry 20*, 6630−6635.
Rall, S. C., Jr., Weisgraber, K. H., Mahley, R. W., Ogawa, Y., Fielding, C. J., Utermann, G., Haas, J., Steinmetz, A., Menzel, H. J., & Assmann, G. (1984) *J. Biol. Chem. 259*, 10063−10070.
Roberts, G. C. K. (1981) in *Standards in fluorescence spectrometry* (Miller, J. N., Ed.) pp 49−67, Chapman and Hall, New York.
Schmidt, H. H. J., Remaley, A. T., Stonik, J. A, Ronan, R., Wellmann, A., Thomas, F., Zech, L. A., Brewer, H. B., Jr., & Hoeg, J. M. (1995) *J. Biol. Chem. 270*, 5469−5475.
Segrest, J. P., Jackson, R. L., Morrisett, J. D., & Gotto, A. M., Jr. (1974) *FEBS Lett. 38*, 247−258.
Segrest, J. P., De Loof, H., Dohlman, J. G., Brouillette, C. G., & Anantharamaiah, G. M. (1990) [published erratum appeared in (1991) *Proteins: Struct., Funct., Genet. 9*, 79]. *Proteins: Struct., Funct., Genet. 8*, 103−117.
Segrest, J. P., Jones, M. K., De Loof, H., Brouillette, C. G., Venkatachalapathi, Y. V., & Anantharamaiah, G. M. (1992) *J. Lipid Res. 33*, 141−166.
Shapiro, J. P., Law, J. H., & Wells, M. A. (1988) *Annu. Rev. Entomol. 33*, 297−318.
Sorci-Thomas, M., Kearns, M. W., & Lee, J. P. (1993) *J. Biol. Chem. 268*, 21403−21409.
Soutar, A. K., Garner, C. W., Baker, H. N., Sparrow, J. T., Jackson, R. L., Gotto, A. M., & Smith, L. C. (1975) *Biochemistry 14*, 3057−3064.
Sparks, D. L., Anantharamaiah, G. M., Segrest, J. P., & Phillips, M. C. (1995) *J. Biol. Chem. 270*, 5151−5157.
Sparrow, J. T., & Gotto, A. M., Jr. (1980) *Ann. N.Y. Acad. Sci. 348*, 187−211.
Srinivas, R. V., Venkatachalapathi, Y. U., Rui, Z., Owens, R. J., Gupta, K. B., Srinivas, S. K., Anantharamaiah, G. M., Segrest, J. P., & Compans, R. W. (1991) *J. Cell. Biochem. 45*, 224−237.
Stanssens, P., Opsomer, C., McKeown, Y. M., Kramer, W., Zabeau, M., & Fritz, H. J. (1989) *Nucleic Acids Res. 17*, 4441−4454.
Swaney, J. B. (1986) *Methods Enzymol. 128*, 613−626.
Utermann, G., Haas, J., Steinmetz, A., Paetzold, R., Rall, S. C., Jr., Weisgraber, K. H., & Mahley, R. W. (1984) *Eur. J. Biochem. 144*, 325−331.
Vanloo, B., Morrison, J., Fidge, N., Lorent, G., Lins, L., Brasseur, R., Ruysschaert, J. M., Baert, J., & Rosseneu, M. (1991) *J. Lipid Res. 32*, 1253−1264.
Vercaemst, R., Union, A., Rosseneu, M., De Craene, I., De Backer, G., & Kornitzer, M. (1989) *Atherosclerosis 78*, 245−250.
Wald, J. H., Goormaghtigh, E., De Meutter, J., Ruysschaert, J. M., & Jonas, A. (1990) *J. Biol. Chem. 265*, 20044−20050.
Yanisch-Perron, C., Vieira, J., & Messing, J. (1985) *Gene 33*, 103−119.
Zhou, C., Yang, Y., & Jong, A. Y. (1990) *BioTechniques 8*, 172−173.

BI951297U